Spurious Diapycnal Mixing of the Deep Waters in an Eddy-Permitting Global Ocean Model

MEI-MAN LEE, ANDREW C. COWARD, AND A. J. GEORGE NURSER

James Rennell Division, Southampton Oceanography Centre, Southampton, United Kingdom

(Manuscript received 7 June 2001, in final form 18 October 2001)

ABSTRACT

Recent idealized studies have shown that both explicit horizontal diffusion and the implicit diffusion associated with the advection scheme in high-resolution *z*-coordinate models may drive unrealistically high rates of diapycnal mixing. The aim here is to see whether the diapycnal mixing associated with the advection scheme in a global eddy-permitting (¼° by ¼°) *z*-level model is sufficiently strong to corrupt the thermohaline circulation. This paper diagnoses the diapycnal fluxes by using the ideas of water mass transformation.

In the Southern Ocean, the model deep and bottom waters drift rapidly away from the Levitus climatology, with dense isopycnals moving downward at rates of up to 35 m yr^{-1}. The strong upward flux (up to 50 Sv) through the dense isopycnals cannot be explained by the incorrect surface forcing (as a result of poor surface fluxes and no ice model) as most of the anomalous diapycnal fluxes are occurring in the deep ocean far from surface forcing. Hence, the excessive diapycnal flux is driven by diffusion in the model, both explicit and implicit.

The ''effective'' diapycnic diffusivity driven by the numerical diffusion (associated with the horizontal advection scheme) is found to be the same order, 1–10 $cm^2\ s^{-1}$, as that driven by the explicit horizontal diffusion. For strong vertical velocities (~20 m day^{-1}) as in models forced by high frequency winds, the vertical advection scheme also gives similar effective diffusivities. These effective diffusivities are considerably greater than suggested by observations. To alleviate these problems, it is suggested that eddy-resolving *z*-level climate models will require 1) less diffusive horizontal advection schemes and 2) better vertical resolution throughout much of the water column.

1. Introduction

In order to give a realistic description of the thermohaline and deep circulation, numerical models need 1) to produce water masses with the correct properties, to 2) transport them correctly, and 3) to operate with realistic rates of mixing so as to maintain the watermass characteristics. If models initialized with realistic deep waters cannot satisfy these requirements, then their deep waters will drift away from reality.

In order to produce the watermasses, the model must be driven by the correct surface fluxes and include an ice model in the deep water formation regions. In order to transport water masses correctly, the model must have sufficient resolution to adequately describe the boundary currents and to develop a realistic, vigorous mesoscale eddy field. Unfortunately, however, the rapid velocities and highly folded tracer fields implied by such high resolution may drive spuriously large mixing rates in a *z*-coordinate model (Roberts and Marshall 1998; Griffies et al. 2000).

Below the surface boundary layer, diapycnic mixing is thought to be driven primarily by breaking internal waves, whose energy derives eventually from wind forcing and tides (Munk and Wunsch 1998). Observed values of diapycnic turbulent diffusivity range from 0.1 $cm^2\ s^{-1}$ (Ledwell et al. 1993) in the thermocline to perhaps 1 $cm^2\ s^{-1}$ (Polzin et al. 1997) in abyssal regions, rising to larger values near rough topography where the internal wave activity is particularly strong as a result of tidal interaction with the topography. A realistic ocean model needs to be able to operate with similar values of diapycnal diffusivity.

This is not a problem for an ''ideal'' isopycnic model with only one active tracer (or with a linear equation of state).[1] In this case, lateral diffusion is by construction on isopycnals, so does not generate diapycnic mixing. Also, diapycnal fluxes in the interior layers are formulated explicitly. There can be no ''numerical'' diapycnal mixing. Finally, these models run stably with arbitrarily small values of diapycnic diffusivity.

Corresponding author address: Dr. Mei-Man Lee, James Rennell Division, Southampton Oceanography Centre, Southampton SO14 3ZH, United Kingdom.
E-mail: mmlee@soc.soton.ac.uk

[1] Realistic isopycnic models with temperature and salinity and a nonlinear equation of state can have problems in handling cabbeling and thermobaricity from which spurious diapycnic mixing might occur.

In contrast, *z*-level models, which are the type of model used most frequently for ''realistic'' eddy-resolving ocean simulations, do not automatically preserve properties along isopycnals.

Explicit diffusion in such models, included to parameterize subgrid-scale processes, has traditionally been horizontal. This gives rise to diapycnal density flux wherever the isopycnals slope, as over western boundary currents and eddies—the ''Veronis effect'' (Veronis 1977). If lateral diffusion is instead performed on isopycnals (Griffies et al. 1998) this spurious diapycnal mixing is much reduced.

However, if the advection scheme is to perform satisfactorily, some smoothing of *all* tracers is necessary and isopycnal diffusion will not smooth the density field. The resolution of grid cells is finite, so both vertical and horizontal advection in a *z*-level coordinate model lead to incorrect propagation (dispersion) of the tracer (and hence density) fields (e.g., Webb et al. 1998b). These errors lead eventually to small-scale numerical noise that must be smoothed by mixing, either as explicit lateral and vertical diffusion (and in the vertical by convective overturning), or implicitly within the advection scheme. For simple centerd difference, Laplacian diffusivities of $O(U\Delta x)$ in the horizontal (here U is the horizontal speed, Δx the grid spacing) and $O(w\Delta z)$ in the vertical (here w is the vertical speed, Δz the vertical grid spacing; or equivalent biharmonic diffusivities) are required in principle to ensure well-behaved fields. Their purpose is not to parameterize real subgrid-scale physics. These large horizontal diffusivities, of course, again drive spuriously large diapycnal diffusion through the Veronis effect. Alternatively, simple upstream advection gives *implicit* numerical diffusivities of the same order. The classic Flux Corrected Transport (FCT) algorithm (Zalesak 1979; Gerdes et al. 1991), which is a blend of upstream and centerd difference, gives numerical diffusivities that, while smaller, are still of this order, and so can still drive a strong Veronis effect (Griffies et al. 2000).

More accurate advection schemes based on higher-order approximations that require less smoothing are now therefore more frequently employed. Schemes such as the Quadratic Upstream Algorithm for Convective Kinematics (QUICK) algorithm (Leonard 1979; Farrow and Stevens 1995) and Modified Split Quick (MSQ) (Webb et al. 1998b) have been implemented in ocean models. The QUICK scheme leaves a truncation error, second order in Δx, formally of the same order as the centerd difference, but only a quarter the size, and includes an implicit velocity-related biharmonic diffusion; while the MSQ scheme is similar, but (apart from the velocity-dependent biharmonic diffusion) is accurate to the fourth order.

Such schemes however still retain considerable numerical diffusivity. Griffies et al. (2000) have documented in some detail the effective diffusivity associated with a variant of QUICK, Quicker (Holland et al. 1998), as well as that associated with a pseudo–fourth-order scheme. They found that in idealized models of vigorously eddying channels, with rapid velocities and highly folded tracer fields, Quicker gave an effective diapycnal diffusivity that scaled as $(\Delta x)^2$, but with a fairly large coefficient. Even with horizontal resolution of ⅛°, the effective implicit diffusivity reached up to 2 $cm^2\ s^{-1}$.

In this contribution we diagnose the diapycnal fluxes in a global eddy-permitting (¼°) model [Ocean Circulation and Climate Advanced Modelling Project (OCCAM); Webb et al. 1998a], which employs the MSQ scheme. Our aims are to see whether the biharmonic mixing included within the advection scheme is sufficiently strong to corrupt the thermohaline circulation and to diagnose the effective diffusivity. The focus is on the ocean thermocline and abyss, away from surface forcing.

We diagnose the model using the idea of water mass transformation (Walin 1982; Speer and Tziperman 1992). This allows us to quantify a net diapycnal flux in the model. This method of analysing diapycnal flux has been applied for instance to isopycnic layer models of the North Atlantic Ocean (Nurser et al. 1999) and the Southern Ocean (Marsh et al. 2000), and a *z*-level model of the North Atlantic (Marshall et al. 1998). It has similarities to the method employed by Griffies et al. (2000).

We consider three runs of the model. One has explicit horizontal diffusivity (as well as the implicit biharmonic diffusion) and so might be expected to have an elevated level of diapycnal diffusivity as a result of the Veronis effect. It is forced by climatological monthly average winds. The second is identical except that it is forced by 6-hourly European Centre for Medium-Range Weather Forecasts (ECMWF) wind fields instead of climatological winds. These result in internal waves with large ($\sim$20 m day^{-1}) oscillating vertical velocities. The resultant ''heaving'' of density surfaces is found to give enhanced diffusive fluxes as a result of the biharmonic diffusion within the MSQ scheme acting on vertical advection. The third run is again forced by climatological winds, but, instead of explicit horizontal diffusivity, employs the Griffies et al. (1998) formulation of isoneutral diffusivity. In this formulation the lateral diffusive flux is oriented along neutral (local isopycnal) surfaces, and so does not drive diapycnal flux. This run should give the smallest effective diffusivity.

The paper is organised as follows. Section 2 gives a brief description of the model, section 3 explains the diagnostic tools to be used and gives the results, and section 4 discusses the implication to eddy-resolving climate models.

2. The model

OCCAM is a *z*-level global ocean model. The model uses finite differences on a horizontal staggered B grid

(Arakawa 1966) to solve the ocean primitive equations. This physical framework owes its origins to the works of Bryan (1969), Semnter (1974), Cox (1984), and the Modular Ocean Model (MOM; Pacanowski 1995). However, the OCCAM model has been rewritten specifically for use on scalar massively parallel processor (MPP) architectures, such as the Cray-T3E (Webb et al. 1997), and incorporates several important developments. In particular, tracers are advected both horizontally and vertically with the modified split QUICK (MSQ) scheme. This involves a fourth-order accurate advection scheme together with a velocity dependent biharmonic diffusion. Other developments include a free-surface and a two-grid system to avoid a singularity at the North Pole (Coward et al. 1994).

The horizontal resolution is everywhere ¼° in each direction. There are 36 vertical levels varying in thickness from 10 m at the surface to 250 m at depth. Full details of the model configuration can be found in Webb et al. (1998a). A quantitative analysis of the model's performance in the Pacific Ocean is given in Saunders et al. (1999).

The model is integrated from rest with initial tracer fields taken from the annual-mean climatology (Levitus et al. 1994). For the first four years of integration the tracer fields are relaxed towards climatological conditions (monthly at the surface and annual elsewhere) with relaxation times of 30 days at the surface and 360 days elsewhere. After these first four years, relaxation is applied to the surface layer (the upper 10 m) only.

For the first four years plus four further years, the model is driven by a set of wind stress fields interpolated from a set of 12 monthly averaged fields derived from ECMWF wind stresses for 1986–88. Over these first eight years the model used normal horizontal Laplacian diffusion (100 $m^2\ s^{-1}$) and viscosity (200 $m^2\ s^{-1}$) to represent lateral mixing. Richardson-number dependent vertical mixing (Pacanowski and Philander 1981) is used for the tracer fields throughout all but the first six months of integration. Away from regions of strong shear this gives vertical diffusivities of $\sim$0.5 $cm^2\ s^{-1}$. Vertical momentum is mixed with constant eddy viscosity of 1 $cm^2\ s^{-1}$.

In this study, we analyze three sets of model state fields. They all start from the same state, at the start of year 8, that is four years after the interior relaxation to climatology has been switched off. The three sets are

- *MON*: Forced by monthly mean winds and with horizontal diffusion as during years 4–8. Data are archived every 15 days over years 8.0–12.0.
- *6HW*: As MON, but forced with 6-hourly wind stresses (ECMWF) from the period 1992 onward. Data are 5-day running means for years 8.0–11.0, archived every 5 days.
- *ISO*: As MON, but using isoneutral diffusion (Griffies et al. 1998). Data are archived every 15 days for years 8.0–12.0.

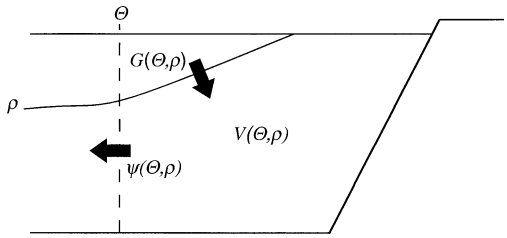

FIG. 1. Schematic meridional sections, showing the diapycnal flux "down" across the ρ isopycnal and south of Θ, $G(\Theta, \rho)$, the volume below the ρ isopycnal and south of Θ, $V(\Theta, \rho)$, and the northward flow of waters denser than ρ across Θ, $\psi(\Theta, \rho)$.

The *z*-level datasets are projected into 72 fixed but unevenly spaced potential density layers (referenced to 2000 m). The density bins chosen are given in appendix A. The depths of the potential density surfaces are determined by linear interpolation from the *z*-level datasets. Transports in the layers lying between the isopycnal surfaces are calculated on the assumption that velocities were uniform through each grid box of the *z*-level model. All averaging to give zonal-means, annual means, etc., is then performed at constant density.

3. Diagnostics

We wish to diagnose the cross-isopycnal "diapycnic" flow in the model. In drifting models, where isopycnals are moving upward or downward, this can be very different from the convergence of the flow below the isopycnal (Wacogne and Pacanowski 1996; Marsh et al. 2000). This is explained below and illustrated in Fig. 1.

We define the meridional streamfunction

$$\psi(\Theta, \rho) = \int_{\theta=\Theta} \int_{z_b}^{z(\rho)} v\, dz\, dl = \int_{\theta=\Theta} \int_{\rho}^{\rho_{\max}} vh\, d\rho\, dl \qquad (1)$$

to be the total transport of waters heavier than ρ across the line of latitude $\theta = \Theta$. Here l is zonal distance, z_b is the bottom, $\rho_{\max}$ the heaviest (bottom) density at that latitude and $h = -\partial z/\partial\rho$, so $h\delta\rho$ is the thickness of the layer sandwiched between the $\rho + \delta\rho$ and ρ isopycnals.

We further write

$$V(\Theta, \rho) = \int_{\theta<\Theta} \int_{z_b}^{z(\rho)} dz\, dA = \int_{\theta<\Theta} \int_{\rho}^{\rho_{\max}} h\, d\rho\, dA \qquad (2)$$

(here dA is the area element) to be the total volume of fluid with density greater than ρ lying south of Θ. Note that $\psi(\Theta, \rho)$ and $V(\Theta, \rho)$ do depend on time, despite not being written with explicit time dependence.

If we then assume incompressibility it follows that the total diapycnal flow across the isopycnal (our sign convention is that "downward" flow from light to heavy

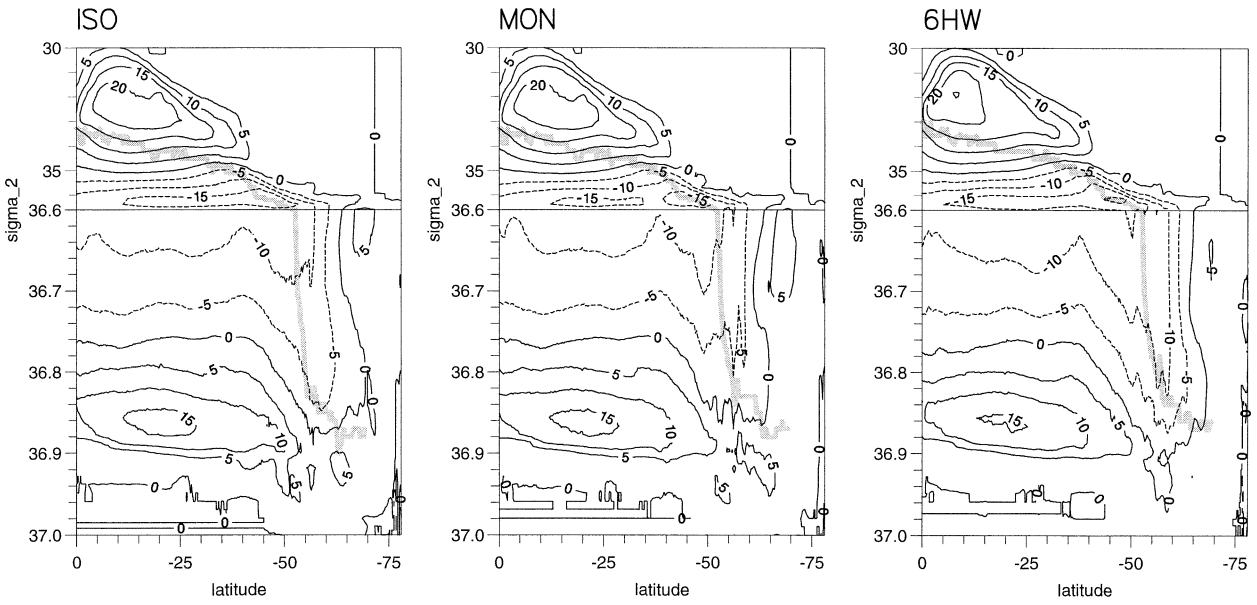

FIG. 2. The time mean meridional streamfunction, $\psi(\Theta, \rho)$ in Sv; contour interval is 5 Sv. The vertical axis for σ_2 greater than 36.6 is expanded for visualization. The thick gray lines indicate the heaviest density at which convective mixing ever occurs at the latitude over the diagnostic period.

is positive) south of $\theta = \Theta$, $G(\Theta, \rho)$, must appear partly as volume inflation, partly as export. Thus,

$$G(\Theta, \rho) = \psi(\Theta, \rho) + \frac{\partial}{\partial t} V(\Theta, \rho). \qquad (3)$$

The G includes the diapycnic flux resulting from diffusive processes and from surface fluxes. In the steady state, all of the flow down across the ρ isopycnal must be exported, with $G(\Theta, \rho) = \psi(\Theta, \rho)$, as noted by Speer (1997). However, the point is that when the inflation rate $\partial V(\Theta, \rho)/\partial t \neq 0$, part of the diapycnal flow may be used to inflate the volume under the ρ isopycnal, so the meridional streamfunction differs from the diapycnic flow, $G(\Theta, \rho) \neq \psi(\Theta, \rho)$.

So there are two streamfunctions, $\psi(\Theta, \rho)$ and $G(\Theta, \rho)$. Both have deficiencies when the density structure is evolving. The meridional streamfunction $\psi(\Theta, \rho)$ gives the correct isopycnal flow but incorrect diapycnal flow. Similarly, the ''diapycnal streamfunction'' $G(\Theta, \rho)$ gives the correct diapycnal flow but incorrect isopycnal flow. The deviation of $G(\Theta, \rho)$ from $\psi(\Theta, \rho)$ gives a measure of the importance of model drift.

These streamfunctions will be diagnosed in the model, using potential density referenced to 2000 m, σ_2. For the purpose of this study, we will restrict ourselves to the Southern Ocean.

a. Meridional transports

The meridional volume transport streamfunction is calculated according to Eq. (1). Volume fluxes are averaged over the period of 4 yr (or 3 yr in the 6HW case). This calculation, of course, includes the contribution of eddy-induced transport from both standing and transient eddies.

The meridional streamfunctions in the three cases are similar (Fig. 2). This suggests (not surprisingly) that over a period of 4 yr the changes in the density structure driven by the inclusion of high-frequency wind forcing or to differing treatment of lateral diffusion are not sufficient to generate greatly different flows.

The usual three cells are present, as in Döös and Webb (1994), Hirst et al. (1996), McIntosh and McDougall (1996), and Marsh et al. (2000). There is 1) a subtropical cell in the lighter density classes ($\sigma_2 < 35$), associated with surface cooling of subtropical waters to form mode waters; 2) a subpolar cell in the intermediate density classes ($35 < \sigma_2 < 36.76$), which we identify as upper North Atlantic Deep Water (NADW, and possibly Upper Pacific Deep Waters) moving southward, lightening, and returning northward as intermediate water; and 3) a deep cell ($36.76 < \sigma_2$) that might be identified as lower NADW and Pacific deep water moving southward, being cooled, and returning northward as Antarctic Bottom Water (AABW).

The subtropical cell has a strength of about 20 Sv (1 Sv $= 10^6$ m^3 s^{-1}), similar to that in other models such as FRAM [(Fine Resolution Antarctic Model), 1/4° resolution; Döös and Webb 1994; McIntosh and McDougall 1996] and a noneddy-resolving 1° resolution run of MICOM [(the Miami Isopycnic Coordinate Model); Marsh et al. 2000].

The subpolar cell carries 15 Sv. There is a flow of upper NADW (and deep Indian and Pacific Ocean waters), southward from the equator to about 40°S, at fairly constant density. Over 40° to 55°–60°S, slightly denser

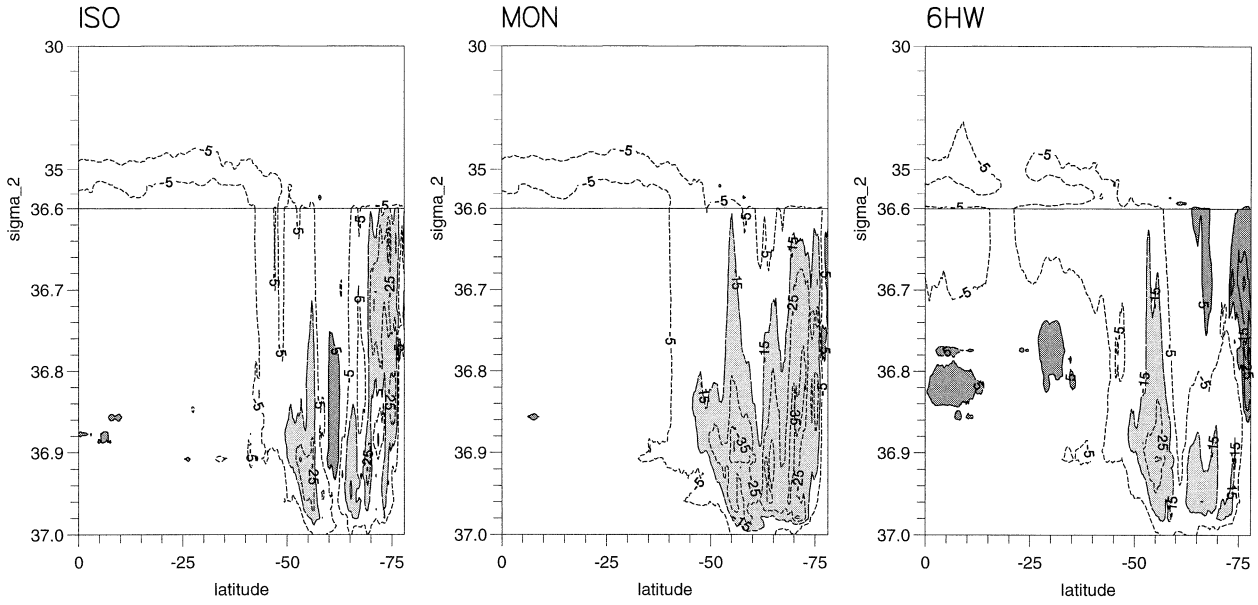

FIG. 3. The rate of change of the height of isopycnal surfaces, $\partial z/\partial t$ (in m yr^{-1}). The contour intervals are 10 m yr^{-1}. The solid lines indicate isopycnals moving upward and broken lines indicate isopycnals moving downward. The light shades are for values less than -15 m yr^{-1} and the dark shades are for values greater than 5 m yr^{-1}.

waters also move south, before the cell closes with apparent lightening to the south. Note that the contours of the streamfunction are seen to be ''sucked down'' around 55°–60°S at $\sigma_2 = 36.9$. This does not necessarily imply diapycnic flux because the model may be drifting as explained in Eq. (3). In other words, we cannot say that there are 5 Sv of NADW being made denser before lightening again.

The bottom cell also transports 15 Sv. Note that using σ_2, potential density referenced to 2000 m, is sufficient to separate the deep water (NADW, etc.) from the bottom water (AABW, etc.), giving results similar to McIntosh and McDougall's (1996) diagnosis of FRAM in terms of neutral density. A formation rate of 15 Sv of bottom waters (defined here as $\sigma_2 < 36.85$) is probably on the low side. Observations give a fairly well-established northward flux of 6–7 Sv in the Atlantic (Schmitz 1996), but the picture in the Indian and Pacific Oceans is less clear. Beal and Bryden (1999) suggest 10 Sv of northward deep [$\gamma > 27.9$, where γ is neutral density (here this is equivalent to $\sigma_2 > 36.85$)] flow in the Indian Ocean across 32°S returning over $27.0 < \gamma < 27.9$ (equivalent to $35.75 < \sigma_2 < 36.85$). Whitworth et al. (1999) diagnose a northward flux of 16 Sv of bottom waters in the Pacific, while Tsimplis et al.'s (1998) inverse analysis finds 12 Sv of bottom water flowing northward across 32°S, returning at intermediate depths, slightly lighter. A rough estimate from their Fig. 13 (which includes no Indonesian throughflow) might be a net northward transport of ~5 Sv of waters with $\sigma_2 > 36.85$. An Indonesian throughflow of ~12 Sv (Schmitz 1996) that is assumed to be supplied barotropically across 32°S would give an extra ~6 Sv, yielding 11 Sv. This would give 17 Sv plus the Indian Ocean contribution (~10 Sv), in total 27 Sv, to compare with the 15 Sv of water $\sigma_2 > 36.85$ flowing north in the model. However, these observational estimate are uncertain. For example, Sloyan and Rintoul (2001) give 50 Sv of deep overturning.

Note that these bottom cells in our model do not extend south of 50°S. The (fairly realistic) northward flow at 40°–50°S is not being replenished by northward flow south of 50°S. The model does not renew the bottom water, because of the poor representation of winter fluxes near Antarctica (Levitus is biased toward summer values by the paucity of winter observations) and the absence of an ice model. This is quite common in ocean models; for example, Marsh et al. (2000) also found that their model failed to form AABW.

b. Model drift

We define the model drift as the rate of change in the heights of isopycnals. Figure 3 shows $dz/dt = (z_{\text{end}} - z_{\text{start}})/\delta t$, where z_{start} and z_{end} are the zonally averaged heights of isopycnals at the start and the end of the analysis period, of length δt. Light shading in Fig. 3 indicates where the heights decrease faster than 15 m yr^{-1}.

In all three cases, there is rapid drift south of 45°S where isopycnal surfaces move downward at a rate of at least 5 m yr^{-1} and at 35 m yr^{-1} in some places. In the MON and ISO cases, almost all the isopycnal surfaces over the whole Southern Ocean move downward. However, with 6HW some lighter isopycnal surfaces

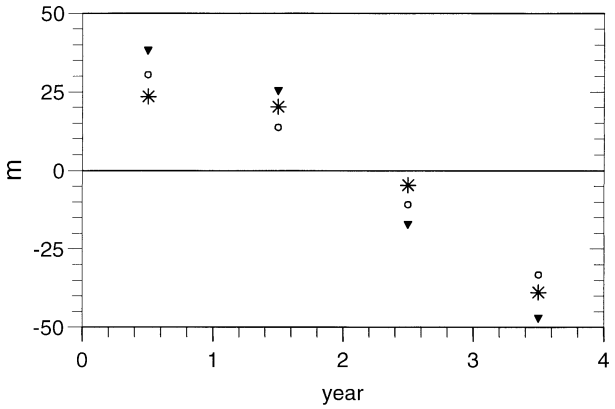

FIG. 4. Anomalies of annual-zonal mean height (in m) of various isopycnals from their 4-yr-zonal mean heights at 56°S in the ISO case. The circles, stars, and triangles are for $\sigma_2 = 36.85$, 36.88, and 36.9.

move upward at low latitudes (north of 40°S) and at high latitudes around 75°S.

In general, the largest downward movements of isopycnals are roughly at $\sigma_2 \sim 36.9$ and between 50°–60°S, associated with the loss of AABW and the gain of upper deep waters. One reason for this is that, as discussed above, the model fails to form AABW. However, the rate of loss of AABW in this model is an order of magnitude larger than that in the isopycnic model of Marsh et al. (2000), whose model also failed to form AABW. This suggests that in our model AABW is also being lost through diapycnic mixing.

This hypothesis is supported by the fact that the ISO case loses dense water masses less rapidly. Isoneutral diffusion is designed to diffuse tracer along neutral surfaces, and so should not drive diapycnal mixing, unlike the horizontal diffusion in MON. The difference between MON and ISO indicates that the explicit horizontal diffusion contributes at least half of the model drift. However there is still considerable drift in ISO, which could be caused by the lack of bottom water formation, vertical diffusion, or, as we shall see, implicit mixing associated with the advection scheme.

The 6HW case also shows a different form of drift in that isopycnic surfaces move *upward* in some places. At latitudes north of 40°S, the volume of water $36.80 < \sigma_2 < 36.85$ increases and the volume of water $36.7 < \sigma_2 < 36.8$ decreases. This implies a volume flux from light to dense isopycnals. We believe (see section 3d) that this additional drift is associated with the strong vertical motions ($\sim 2 \times 10^{-2}$ cm s^{-1}) due to the internal waves generated at the surface by the high frequency forcing (Fox and Haines 2000).

Being an eddy-permitting model, the isopycnic surfaces also move up and down in all the runs when eddies pass through. To be sure that the height changes in Fig. 5 are a sign of long term drift rather than some random fluctuation, in Fig. 4 we plot the year-on-year movement of the annual-zonal mean heights of a selection of isopycnals at latitude 56°S from the ISO case ($\sigma_2 = 36.85$, 36.88, and 36.9). These isopycnal surfaces deepen steadily year on year, falling 100 m over the 4 yr, as we would expect from a steady drift.

c. Diapycnal flux

The zonally integrated and time-averaged diapycnal streamfunction $G = \psi + \partial V/\partial t$ is plotted in Fig. 6, the sum of the meridional streamfunction (Fig. 2) and the

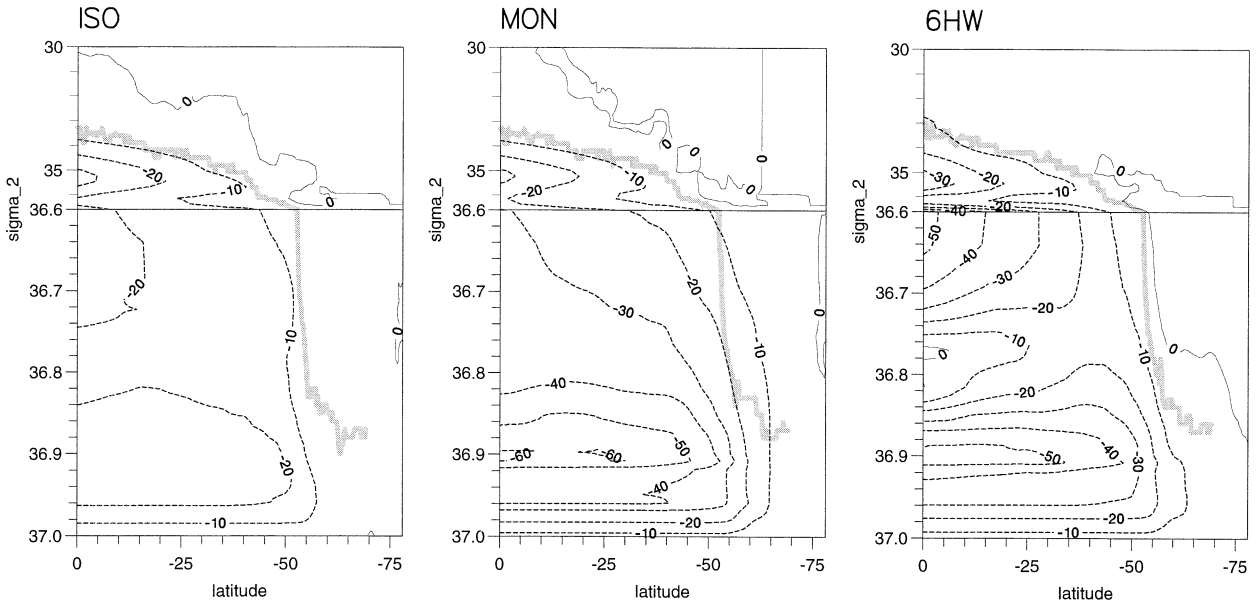

FIG. 5. The rate of change of $V(\Theta, \rho)$, $\partial V(\Theta, \rho)/\partial t$ (in Sv). Contour interval is 10 Sv.

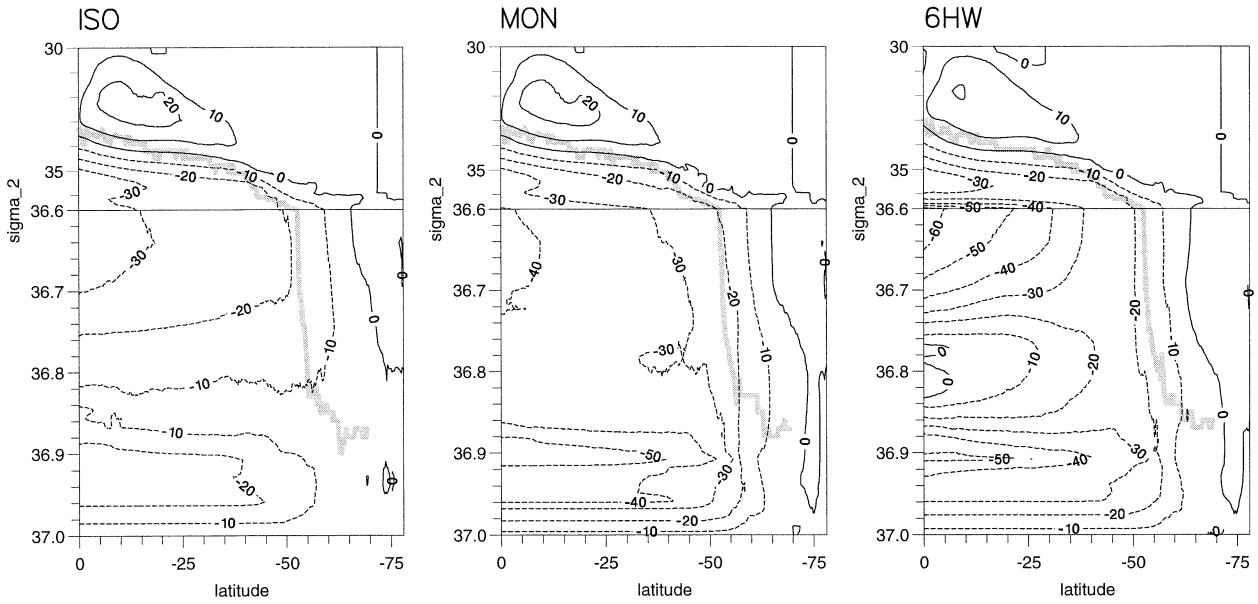

FIG. 6. Diapycnal streamfunction, $G(\Theta, \rho)$ (in Sv). Contour interval is 10 Sv.

rate of volume change below the isopycnal, $\partial V/\partial t$ (Fig. 5). Note that the diapycnal flux per unit latitude is simply $\partial G/\partial\Theta$.

Comparing Figs. 2, 5, and 6, it is evident that, except on the very light isopycnals ($\sigma_2 < 34$), the diapycnal streamfunction is dominated by the model drift. In fact the model drift is so severe that the diapycnal flux deduced from the meridional transport streamfunction alone gives a misleading picture of the actual diapycnal flux in the model. For example, in the MON case, there is as much as 50-Sv diapycnal volume flux of bottom to deep water across $\sigma_2 \sim 36.9$, south of 40°S. This flux is from dense to light, opposite to that implied by the meridional streamfunction. Even a fairly light ($\sigma_2 \sim 35$) isopycnal within the intermediate waters has 30 Sv moving ''upward'' through it (Fig. 6), which is almost all associated with model drift (Fig. 5).

Comparison of the MON and ISO cases in Fig. 6 suggests that the horizontal diffusion in the MON case drives at least 30 Sv of the diapycnal flux across $\sigma_2 \sim 36.9$, more than half of the total. There is however little difference between the two runs for the intermediate waters ($35 < \sigma_2 < 36$). Across the ''core'' of the NADW, at $\sigma_2 \sim 36.7$, the flux is reduced by a quarter to 30 Sv in ISO as against 40 Sv in MON.

The diapycnal flux in the 6HW case is the strongest of all. The upward flux across the light NADW/intermediate water isopycnal $\sigma_2 \sim 36.64$ now exceeds 60 Sv. There is also a cell within the NADW, north of 45°S, where 20 Sv flows downward (from light to dense) across $\sigma_2 \sim 36.8$; this is associated with the upward movement of this isopycnal seen in Fig. 3. In the next section we show that these additional diapycnal fluxes result from the biharmonic mixing in the numerical scheme stimulated by the strong vertical velocities of the internal waves.

Diapycnal flow is driven in general by diffusive processes and by surface fluxes. The diapycnal fluxes in Fig. 6, even with isopycnal diffusion, are clearly unable to support the (fairly realistic) thermohaline circulation implied by the meridional streamfunction in Fig. 2, or indeed any plausible thermohaline circulation. So the question is, are these diapycnal fluxes ''wrong'' because there is too much mixing in the model, or are they wrong because the surface fluxes are wrong?

We believe that they are wrong primarily because there is too much mixing in the model. Even in case ISO there is 10–15 Sv of flow across the $\sigma_2 \sim 36.94$ isopycnal north of 60°S, and the ~20 Sv of flow across $\sigma_2 \sim 36.65$ north of 50°S. These flows occur where these isopycnals still lie deep, far from the surface, and so must be ascribed to diffusion. Even if bottom waters were being formed satisfactorily, we believe that these unrealistic diapycnal flows would still occur in the model. In the next section, we attempt to estimate how plausible these fluxes are by estimating an ''effective diapycnal diffusivity.''

We plot (Fig. 7a) the field of (downward) diapycnal velocity on the $\sigma_2 = 36.9$ isopycnal for the ISO run, calculated as the divergence of the horizontal transport below the isopycnal, less the (downward) rate of drift of the isopycnal. Due to numerical discretization errors, the field of the divergence of the transport below the isopycnal is very noisy at the full model resolution of ¼°, so this field is smoothed by averaging over a 1° grid. Values of diapycnic velocity reach about 100 m yr^{-1}, in both senses; note that there is more downward motion than upward, consistent with the zonal average

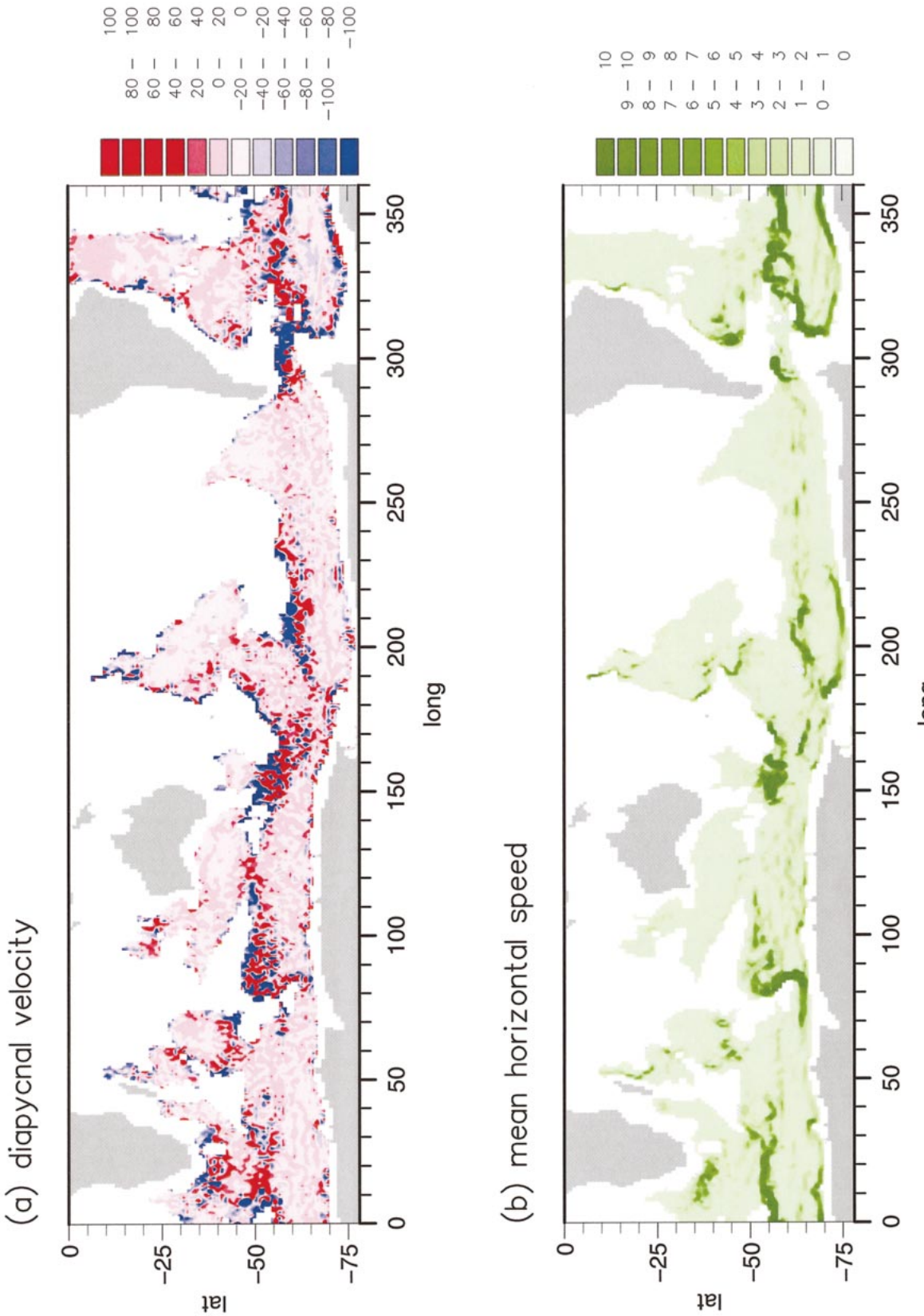

FIG. 7. For the ISO case: (a) field of diapycnal velocity (in m yr^{-1}; positive is downward) across $\sigma_2 = 36.9$; (b) time-mean horizontal speed (in cm s^{-1}) at the same isopycnal.

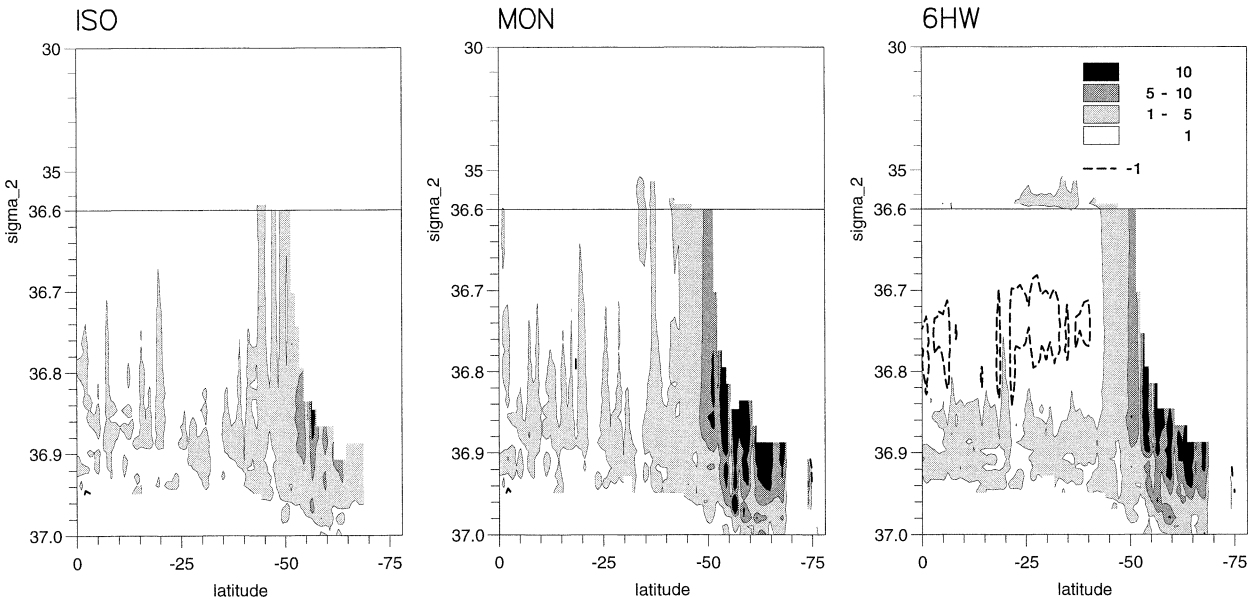

FIG. 8. Effective diffusivity, κ_e (in cm^2 s^{-1}), below the convective mixing regions (i.e., the gray lines in Fig. 2). Note the negative values (broken lines) in the 6HW case. The light, dark and black shades are for values greater than 1, 5, and 10 cm^2 s^{-1} respectively.

Fig. 6. There is good correlation between diapycnic flux and the path of the Antarctic Circumpolar Current (ACC) and boundary currents, as shown in the field of mean horizontal speed (Fig. 7b). This is consistent with the hypothesis that the diapycnic flux is associated with the advection scheme.

d. Effective diffusivity

We estimate an effective diapycnal diffusivity, κ_e, a function of density and latitude, by relating the zonally and time-averaged diffusive density flux to the mean stratification [see appendix B; in particular, Eq. (B6)]. The diffusive density flux across a given isopycnal is assumed to be equal to the integrated density change below the isopycnal, which is calculated by integrating the diapycnal velocities over all densities greater than that density. Surface processes are excluded by considering only the region below the surface convective layer.

This method of calculating the diffusive flux is admittedly imperfect since both the convergence of the meridional diffusive flux and cabbeling are ignored (see appendix B for more details). North of 40°S the mean meridional density gradient is small and so the meridional diffusive flux is not important. Over the ACC it is substantial, and its convergence acts as a density source/sink on the northern/southern flank of the ACC. Neglecting this term thus causes us to underestimate/overestimate the diffusivity over northern/southern ACC where the term acts as a density source/sink. On the other hand, cabelling always acts as a density source, so its neglect results an overestimate of diffusivity.

However, the broad picture is fairly robust. Effective diffusivities κ_e in the present model (Fig. 8) exceed 1 cm^2 s^{-1} (light shades) over a substantial fraction of where $\sigma_2 > 36.7$ in all three runs, and exceed 5 cm^2 s^{-1} between 50° and 70°S in all but the ISO case. Note that the high values of apparent κ_e seen south of 60°S in Fig. 8 may result from the (divergent) meridional density flux; however, over the northern flank of the ACC our κ_e may be an underestimate. These effective diffusivities can be compared to the explicit vertical diffusivity κ_m used in the model, which is based on Pacanowski and Philander (1981). Diagnosing κ_m (not shown) from the time-mean field shows $\kappa_m = 0.5$ cm^2 s^{-1} almost everywhere both in the thermocline and the abyss.

Much of this diapycnic diffusion in MON and 6HW can be ascribed to the Veronis effect (Veronis 1977), resulting from explicit horizontal diffusive flux crossing isopycnals. For the horizontal component of the density flux is

$$\mathbf{D}_h = -\kappa_h \boldsymbol{\nabla}_h \rho, \tag{4}$$

where κ_h is the horizontal diffusivity and $\boldsymbol{\nabla}_h = (\partial/\partial x, \partial/\partial y)$ is the horizontal gradient. The resulting diapycnic flux associated with the horizontal flux is $D_{\text{diap}} = \mathbf{D}_h \cdot \boldsymbol{\nabla}_h z$, where z is the isopycnal height. The implied effective diapycnal diffusivity is given by

$$D_{\text{diap}} = -\kappa_{e,d} \frac{\partial \rho}{\partial z}. \tag{5}$$

Thus,

$$\kappa_{e,d} = \kappa_h |\boldsymbol{\nabla}_h z|^2. \tag{6}$$

The point is that this is often quite large, since eddy slopes, $|\boldsymbol{\nabla}_h z|$, in the ACC are frequently $O(5 \times 10^{-3})$. Then, if the isopycnal slope is $n \times 10^{-3}$, $\kappa_{e,d} \sim n^2$ cm^2

s^{-1}. This easily gives the effective diffusivities of 1–10 $cm^2\ s^{-1}$ seen in the model.

The ISO case shows smaller diffusivities, with a significantly reduced region of diffusivity greater than 5 $cm^2\ s^{-1}$ (dark shading). This is consistent with the weaker diapycnal velocities seen in this run. However, both the diapycnal fluxes and diffusivities remain of the same order as in MON (perhaps a half to two thirds), considerably greater than could be expected from the explicit vertical diffusivity alone. This difference between κ_e and κ_m must then either result from advection-scheme mixing or from the isoneutral diffusion scheme—this might be causing some mixing both because σ_2 differs from the neutral density, and also because the scheme allows diapycnal mixing in the bottom grid box. In order to exclude these latter possibilities, the model was run for a short time without either isoneutral or lateral diffusion. This gave diapycnal fluxes and hence diffusivities very similar to the run with isoneutral diffusion. Hence the excess diapycnal diffusion here in case ISO must be induced by the advection scheme. So, it appears that the advection scheme generates diapycnic flux of the same strength as would be generated by an effective diffusivity of order $\geq 1\ cm^2\ s^{-1}$; comparable to that driven by the Veronis effect associated with explicit lateral diffusion of 100 $m^2\ s^{-1}$ as estimated following (6).

These estimates are consistent with simple scaling analysis of the velocity-dependent horizontal biharmonic diffusion term associated with the MSQ advection scheme. The x component of the density flux is (Webb et al. 1998b)

$$D_x = \frac{1}{16}\Delta x^3 |u| \frac{\partial^3 \rho}{\partial x^3}, \tag{7}$$

where Δx is the horizontal grid spacing, here $1–3 \times 10^4$ m, and $|u|$ is a typical velocity, here $10^{-1}\ m\ s^{-1}$.

If we assume that variability in ρ is essentially oscillatory at constant height—that is, associated with a stream of eddies—then it follows that

$$\frac{\partial^3 \rho}{\partial x^3} \sim -L^{-2}\frac{\partial \rho}{\partial x}, \tag{8}$$

where L is some length scale. Thus, the effective horizontal diffusivity, $\kappa_{e,h}$, is given by

$$D_x = -\kappa_{e,h}\frac{\partial \rho}{\partial x}. \tag{9}$$

So,

$$\kappa_{e,h} = \frac{1}{16}\Delta x |u| \left(\frac{\Delta x}{L}\right)^2. \tag{10}$$

Unfortunately the worst case in which the length scale $L \sim \Delta x$ is reasonable for mesoscale eddies, since the Rossby radius is $\sim 2.10^4$ m. Hence $\kappa_{e,h} \sim 100\ m^2\ s^{-1}$, the same order as the explicit horizontal diffusivity in case MON ($100\ m^2\ s^{-1}$). This again then drives a diffusive flux across the sloping isopycnals—a Veronis effect, giving an effective diffusivity of order 1–10 $cm^2\ s^{-1}$. This implies that the advection scheme is generating as much diapycnic flux as the explicit vertical diffusion, or even more in some places. This conclusion is consistent with the findings of Griffies et al. (2000).

In the 6HW case, there are negative diffusivities (upgradient fluxes of density) across $\sigma_2 = 36.7$ at low latitudes. Such upgradient fluxes are known to occur as a result of convection operating on spurious small-scale vertical structure generated by vertical advection with a centerd difference scheme (e.g., Griffies et al. 2000). Here, however, the explanation is that the strong vertical velocities ($\sim 20\ m\ day^{-1}$) associated with the internal waves imply a substantial vertical biharmonic diffusivity. The associated biharmonic density flux is proportional to $+\partial^3\rho/\partial z^3$ (the sign is positive for biharmonic diffusion). Negative diffusivities occur where the density gradient and $\partial^3\rho/\partial z^3$ have the same sign. The density gradient $\partial\rho/\partial z$ is always negative, as otherwise it is convectively unstable. At the same time, $\partial^3\rho/\partial z^3$ can be negative, as it would be either for an exponential type of stratification or for small-scale sinusoidal wiggles (producing alternating signs of $\partial^3\rho/\partial z^3$) superposed upon an ambient constant stratification.

A scaling argument similar to that applied to the horizontal mixing implies an effective vertical diffusivity

$$\kappa_{e,v} \sim \frac{1}{16}\Delta z |w| \left(\frac{\Delta z}{D}\right)^2. \tag{11}$$

Here Δz is the vertical grid spacing and D is the vertical scale of variation. Maximum diffusivities for $D \sim \Delta z$ are then (1/16) $\Delta z |w|$, so for vertical velocities $\sim 2 \times 10^{-4}\ m\ s^{-1}$ ($20\ m\ day^{-1}$, such as occur in the 6HW run with internal waves), and $\Delta z \sim 100$ m, $\kappa_{e,v} \sim \pm 10\ cm^2\ s^{-1}$. Inspection of typical density profiles shows values of $\partial^3\rho/\partial z^3$ which are indeed sufficient, combined with typical internal wave vertical velocities of $\sim 20\ m\ day^{-1}$, to produce negative vertical diffusivities of approximately -5 to $-8\ cm^2\ s^{-1}$ in places. After zonal averaging, this leads to the smaller values seen in Fig. 8.

The vertical biharmonic fluxes are much less important in the other cases MON and ISO without significant internal waves. Here, the vertical velocities are at least an order of magnitude less, giving diffusivities $\kappa_{e,v} \leq 1\ cm^2\ s^{-1}$. Therefore, the systematic effect of this vertical mixing is less than that from the horizontal mixing.

4. Discussion and conclusions

The model has been initialized from the Levitus hydrography. About 10 years later the model density structure is still close enough to climatology that the thermohaline circulation implied by the overturning streamfunction looks plausible. However, the model's deep and bottom waters are drifting away from the Levitus cli-

matology fairly rapidly, with dense isopycnals in the Southern Ocean moving downward at rates of up to 35 m year^{-1}. We have diagnosed the diapycnal volume flux from the divergence of the volume transport below the isopycnal and the rate of drift of the isopycnals. We introduce the ''diapycnal streamfunction,'' a function of density and latitude, to be the flow across the density surface integrated everywhere south of the latitude. Where the model is in steady state, this reduces to the zonally integrated meridional transport streamfunction on density surfaces.

Our diagnosed diapycnal streamfunction shows strong upward flux (up to 50 Sv) through the dense isopycnals. This diapycnal flux is inconsistent with that implied by the meridional streamfunction, if the model were in steady state. Hence this diapycnal flux is driving rapid model drift. If the model were run for a few decades, we doubt that the thermohaline circulation would still be realistic. The absence of correct surface forcing (as a result of poor surface fluxes and no ice model) is not sufficient to explain this ''incorrect'' diapycnal flux, as most of the anomalous diapycnal fluxes are occurring in the deep ocean far from surface forcing. This suggests that the model diapycnal flux is driven by excessive diffusion in the model, both explicit and implicit.

This hypothesis is supported by our diagnosis of ''effective diffusivity.'' In the run MON that included explicit horizontal diffusivity of 100 m^2 s^{-1}, zonally averaged values of this effective diapycnic diffusivity reach 1–10 cm^2 s^{-1} over much of the ACC latitude range. The run (case ISO) with the Griffies et al. (1998) isopycnal diffusion scheme instead of horizontal mixing retains about half to two thirds of the mixing-driven ''upward'' diapycnal flux, reaching 20–30 Sv, and we estimate effective diffusivities, though smaller, still reach 1–10 cm^2 s^{-1}. These diffusivities result primarily from the biharmonic mixing implicit in the advection scheme. They are considerably larger than the explicit vertical diffusivity of 0.5 cm^2 s^{-1}. Note also that we have neglected the effect of cabelling in making our estimate of diffusivity, which is therefore on the low side (see appendix B). This effective diffusivity is nonetheless considerably greater than that suggested by observations. The diapycnic flux driven by it is clearly causing rapid drifting of the deep water properties away from climatology.

Successful eddy-resolving climate models will require less diffusion. It might be argued that higher horizontal resolution should lessen the problem, given that the effective horizontal diffusivity is $O(\Delta x^3 L^{-2} U) \leq O(\Delta x U)$. However, this is only partly true. As found by Roberts and Marshall (1998) and Griffies et al. (2000), an increase in horizontal resolution coupled with a reduction in viscosity leads to more vigorous eddies (larger U), and more finescale structure (filaments, etc., so smaller L). If viscosity is not reduced, the great computational cost of higher horizontal resolution is being paid without gaining the benefit of a more realistic, vigorous eddy field. A more promising approach might be to ensure that the smoothing of the density field in the advection scheme is adiabatic in a manner similar to using thickness diffusion rather than horizontal diffusion (Gent and McWilliams 1990; Roberts and Marshall 1998).

There are also problems associated with the vertical advection. These are most pronounced in the 6HW case, in which high frequency surface forcing generates internal waves, which drive rapid oscillatory vertical motions ($\sim 2 \times 10^{-2}$ cm s^{-1}). These large vertical velocities imply considerable vertical biharmonic flux, with effective diffusivities again reaching 1–10 cm^2 s^{-1}. However, frequently these fluxes are downward (*up* the density gradient). The vertical biharmonic fluxes are less important in the other cases MON and ISO without internal waves where vertical velocities are at least an order of magnitude less.

The problem of vertical advection and mixing in a z-level model is less easy to deal with than the horizontal advection, since an adiabatic formulation in the vertical is not possible. Removing biharmonic diffusion and returning to simple centerd difference generates gridscale noise, which is then smoothed by convection in an equally unphysical manner (Griffies et al. 2000). Instead we suggest that increases in vertical resolution should reduce the w-dependent biharmonic diffusion, which is $\leq O(\Delta z W)$, to tolerable levels. For geostrophic turbulence is largely two-dimensional. Hence finer vertical resolution does not have the same effect in generating stronger vertical velocities as does finer horizontal resolution in increasing horizontal velocities. If then we assume in (11) a vertical depth scale D for variation of ρ of 100 m, a vertical velocity of 20 m day^{-1}, and require the implied diffusivity to be $\sim$0.1 cm^2 s^{-1}, this implies that we require grid boxes of thickness $\Delta z \sim 20$ m.

Climate studies rely on accurate representation of the thermohaline circulation. Since this is sensitive to diapycnal mixing, it is essential that models can operate with realistic levels of mixing. In this paper, we have shown that the diapycnal mixing implied by the advection scheme in a global eddy-permitting model is causing severe drifting of the deep water properties from climatology. If eddy-resolving z-level ocean models are to operate with realistic diapycnic diffusivity, they require more adiabatic horizontal advection schemes. Moreover, if the vertical velocities are strong (e.g., the model includes internal waves) they probably also require higher vertical resolution through much of the water column.

Acknowledgments. We acknowledge useful conversations with David Webb and the assistance of Harry Bryden and Stuart Cunningham in interpreting the observational literature concerning deep flows. We thank Beverly de Cuevas for some of the model runs. Mei-Man Lee and Andrew Coward are partly supported by the EU MAST-3 program TRACMASS CT970142.

APPENDIX A

Density Classes

$\sigma_{2,\min}$	$\sigma_{2,\max}$	Interval
0.00	10.00	10.00
10.00	21.00	11.00
21.00	30.00	3.00
30.00	33.00	0.50
33.00	36.00	0.30
36.00	36.40	0.10
36.40	36.70	0.05
36.70	37.03	0.01
37.03	37.73	0.10
37.73		

APPENDIX B

Calculation of the Effective Diffusivity

To begin, we link the diffusive density flux to the diapycnal volume fluxes. We restrict ourselves to the interior, well away from regions where surface forcing or convection. In these regions, the (potential) density changes can either be due to diffusive density flux or to cabbeling. Thus,

$$\frac{D\rho}{Dt} = -\nabla \cdot \mathbf{D} + C, \tag{B1}$$

where $D/Dt = \partial/\partial t + \mathbf{u} \cdot \nabla$ is the material derivative, $\mathbf{D} = (D_x, D_y, D_z)$ is the ''diffusive density flux'' and C is the cabbeling.

Now the diapycnal velocity, g, is related to the material rate of change of density by

$$g = -\frac{D\rho}{Dt}\frac{\partial z}{\partial \rho}, \tag{B2}$$

where z is the isopycnal height. Integrating from the ocean floor z_b up to the isopycnal ρ [height $z(\rho)$] gives

$$\int_{\rho_{\max}}^{\rho} g \, d\rho = \int_{z_b}^{z(\rho)} \frac{D\rho}{Dt} \, dz, \tag{B3}$$

where $\rho_{\max}$ is the density on the ocean floor. Equation (B3) states that the integral of g over ρ is equal to the total density gain underneath the isopycnal.

From the definition of the diapycnal streamfunction $G(\Theta, \rho)$, it can be seen that $\partial G/\partial y$ (writing $\partial/\partial y = R^{-1}\partial/\partial\Theta$, where R is the radius of earth) gives the diapycnal flow across ρ integrated along the latitude $\theta = \Theta$:

$$\frac{\partial G}{\partial y} = \int_{\theta=\Theta} g \, dl. \tag{B4}$$

Integrating (B4) also from the ocean floor up to the isopycnal ρ then gives

$$\begin{aligned}\int_{\rho_{\max}}^{\rho} \frac{\partial G}{\partial y} \, d\rho &= \int_{\theta=\Theta}\int_{z_b}^{z(\rho)} \frac{D\rho}{Dt} \, dz \, dl \\ &= -\int_{\theta=\Theta} \mathbf{D} \cdot \mathbf{n} \, dl - \frac{\partial}{\partial y}\int_{\theta=\Theta}\int_{z_b}^{z(\rho)} D_y \, dz \, dl \\ &\quad + \int_{\theta=\Theta}\int_{z_b}^{z(\rho)} C \, dz \, dl,\end{aligned} \tag{B5}$$

where we have used (B1) for the density tendency and $\mathbf{n} = (-\partial z/\partial x, -\partial z/\partial y, 1)$ is the upward vector normal (from dense to light) to the ρ surface. Equation (B5) states that zonally integrated density gain over the ρ isopycnal is achieved by (i) downward diffusive flux of density across the isopycnal, (ii) convergence of meridional density flux below the isopycnal, and (iii) cabbeling.

Our aim is to define a diapycnal diffusivity, κ_e, as

$$-\kappa_e \int_{\theta=\Theta} \overline{\frac{\partial \rho}{\partial z}}^{t} \, dl = \int_{\theta=\Theta} \overline{\mathbf{D} \cdot \mathbf{n}}^{t} \, dl, \tag{B6}$$

where $\overline{\ }^{t}$ is time averaging. Using (B5) to replace the right-hand side of (B6), we have

$$\kappa_e = \frac{-\overline{\int_{\rho_{\max}}^{\rho} \frac{\partial G}{\partial y} \, d\rho}^{t} - \frac{\partial}{\partial y}\int_{\theta=\Theta}\int_{z_b}^{z(\rho)} \overline{D_y}^{t} \, dz \, dl + \int_{\theta=\Theta}\int_{z_b}^{z(\rho)} \overline{C}^{t} \, dz \, dl}{-\int_{\theta=\Theta} \overline{\frac{\partial \rho}{\partial z}}^{t} \, dl}. \tag{B7}$$

Our diagnostics calculate the $\partial G/\partial y$ term in (B7); that is, the zonally integrated time average density gain. Unfortunately, we know neither the cabbeling field C nor the horizontal divergence of the diffusive flux. We therefore must neglect both these terms, and use the approximate form

$$\kappa_e \sim \overline{\int_{\rho_{\max}}^{\rho} \frac{\partial G}{\partial y} \, d\rho}^{t} \Bigg/ \int_{\theta=\Theta} \overline{\frac{\partial \rho}{\partial z}}^{t} \, dl. \tag{B8}$$

The question then is: how valid an approximation is (B8)? Cabbeling can be significant, but so long as diffusive temperature fluxes are downgradient, it is always

a density source [is positive in (B7)]. So neglecting this term causes (B8) to *underestimate* κ_e. Another way of seeing this is that we are assuming in (B8) that the density content change under the isopycnal (the G term) is achieved by diapycnal diffusion. Since diapycnal diffusion acts as a density sink (for positive κ_e), neglect of the cabbeling term (a density source) is neglecting the extra diffusion which is necessary to remove this density gain—causing us to underestimate κ_e.

The horizontal diffusive density flux is consistently northwards over the Southern Ocean, and is strongest where the isopycnal slopes are steepest, over the ACC core. The convergence thus acts as a density source over the northern flank of the ACC and a density sink to the south of the ACC. By the same argument as above, then, neglecting this term causes us to underestimate κ_e on the northern flank of the ACC, and overestimate it to the south. North of the ACC the mean meridional density gradient is small and this term becomes less important.

A scaling analysis shows that this term has magnitude of order $(S_m D/L)/S_t^2$ relative to that of the diapycnal flux driven by the Veronis effect as estimated by (9) and (10) in section 3. Here S_m is the time-zonal mean of the isopycnals (maximum values in the mid-ACC may reach 2×10^{-3}), D is half the ocean depth (2000 m), L is the meridional scale of variation of the mean slope ($\sim 10^{\circ} \sim 10^{6}$ m), and S_t^2 is the *total* (mean + eddy) squared slope (values reach 10^{-5}). This parameter reaches order 1 in the ACC, but to the north is small.

REFERENCES

Arakawa, A., 1966: Computational design for long-term numerical integration of the equations of fluid motion: Two-dimensional incompressible flow. Part 1. *J. Comput. Phys.*, **1,** 119–143.

Beal, L. M., and H. L. Bryden, 1999: The velocity and vorticity structure of the Agulhas Current at 32 degrees S. *J. Geophys. Res.*, **104,** 5151–5176.

Bryan, K., 1969: A numerical method for the study of the circulation of the world ocean. *J. Comput. Phys.*, **4,** 347–376.

Coward, A. C., P. D. Killworth, and J. R. Blundell, 1994: Tests of a two-grid world ocean model. *J. Geophys. Res.*, **99,** 22 725–22 735.

Cox, M. D., 1984: A primitive equation 3-dimensional model of the ocean. GFDL/NOAA Ocean Group Tech. Rep. 1, 143 pp. [Available from Princeton University, Princeton, NJ 08542.]

Döös, K., and D. J. Webb, 1994: The Deacon cell and the other meridional cells of the Southern Ocean. *J. Phys. Oceanogr.*, **24,** 429–442.

Farrow, D. E., and D. P. Stevens, 1995: A new tracer advection scheme for Bryan and Cox type ocean general circulation models. *J. Phys. Oceanogr.*, **25,** 1731–1741.

Fox, A. D., and K. Haines, 2000: Modelling internal waves with a global ocean model. *Int. WOCE Newslett.*, **39,** 27–30.

Gent, P. R., and J. C. McWilliams, 1990: Isopycnal mixing in ocean circulation models. *J. Phys. Oceanogr.*, **20,** 150–155.

Gerdes, R., C. Köberle, and J. Willebrand, 1991: The influence of numerical advection schemes on the results of ocean general circulation models. *Climate Dyn.*, **5,** 211–226.

Griffies, S. M., A. Gnanadesikan, R. C. Pacanowski, V. D. Larichev, J. K. Dukowicz, and R. D. Smith, 1998: Isoneutral diffusion in a z-coordinate ocean model. *J. Phys. Oceanogr.*, **28,** 805–830.

——, R. C. Pacanowski, and R. W. Hallberg, 2000: Spurious diapycnal mixing associated with advection in a z-coordinate ocean model. *Mon. Wea. Rev.*, **128,** 538–564.

Hirst, A. C., D. R. Jackett, and T. J. McDougall, 1996: The meridional overturning cells of a world ocean model in neutral density coordinates. *J. Phys. Oceanogr.*, **26,** 775–791.

Holland, W. R., J. C. Chow, and F. O. Bryan, 1998: Application of a third-order upwind scheme in the NCAR ocean model. *J. Climate*, **11,** 1487–1493.

Ledwell, J. R., A. J. Watson, and C. S. Law, 1993: Evidence for slow mixing across the pycnocline from an open-ocean tracer-release experiment. *Nature*, **364,** 701–703.

Leonard, B. P., 1979: A stable and accurate convective modelling procedure based on quadratic interpolation. *Comput. Methods Appl. Mech. Eng.*, **19,** 59–98.

Levitus, S., R. Burgett, and T. P. Boyer, 1994: *Salinity.* Vol. 3, *World Ocean Atlas 1994*, NOAA Atlas NESDIS 3, 99 pp.

Marsh, R., A. J. G. Nurser, A. P. Megann, and A. L. New, 2000: Water mass transformation in the Southern Ocean of a global isopycnal coordinate GCM. *J. Phys. Oceanogr.*, **30,** 1013–1045.

Marshall, J., D. Jamous, and J. Nilsson, 1998: Reconciling thermodynamic and dynamic methods of computation of water-mass transformation rates. *Deep-Sea Res. Part I*, **46,** 545–572.

McIntosh, P. C., and T. J. McDougall, 1996: Isopycnal averaging and the residual mean circulation. *J. Phys. Oceanogr.*, **26,** 1655–1660.

Munk, W., and C. Wunsch, 1998: Abyssal recipes II: Energetics of tidal and wind mixing. *Deep Sea Res. Part I*, **45,** 1977–2010.

Nurser, A. J. G., R. Marsh, and R. G. Williams, 1999: Diagnosing water mass formation from air-sea fluxes and surface mixing. *J. Phys. Oceanogr.*, **29,** 1468–1487.

Pacanowski, R. C., 1995: MOM 2 documentation, user's guide and reference manual. GFDL Ocean Group Tech. Rep. 3, 232 pp. [Available from Princeton University, Princeton, NJ 08542.]

——, and S. G. H. Philander, 1981: Parameterization of vertical mixing in numerical models of tropical oceans. *J. Phys. Oceanogr.*, **11,** 1443–1051.

Polzin, K. L., J. M. Toole, J. R. Ledwell, and R. W. Schmitt, 1997: Spatial variability of turbulent mixing in the abyssal ocean. *Science*, **276,** 93–96.

Roberts, M., and D. Marshall, 1998: Do we require adiabatic dissipation schemes in eddy-resolving ocean models? *J. Phys. Oceanogr.*, **28,** 2050–2063.

Saunders, P. M., A. C. Coward, and B. A. de Cuevas, 1999: The circulation of the Pacific Ocean seen in a Global Ocean Model (OCCAM). *J. Geophys. Res.*, **104,** 18 281–18 299.

Schmitz, W. J., 1996: On the World Ocean circulation: Volume II. The Pacific and Indian Oceans: A global update. Woods Hole Oceanogr. Inst. Tech. Rep. WHOI-96-08, 237 pp.

Semtner, A. J., 1974: A general circulation model for the World Ocean. University of California, Los Angeles, Dept. Meteor. Tech. Rep. 9, 99 pp.

Sloyan, B. M., and S. R. Rintoul, 2001: The Southern Ocean limb of the global deep overturning circulation. *J. Phys. Oceanogr.*, **31,** 143–173.

Speer, K. G., 1997: A note on average cross-isopycnal mixing in the North Atlantic ocean. *Deep-Sea Res. Part I*, **44,** 1981–1990.

——, and E. Tziperman, 1992: Rates of water mass formation in the North Atlantic Ocean. *J. Phys. Oceanogr.*, **22,** 93–104.

Tsimplis, M. N., S. Bacon, and H. L. Bryden, 1998: The circulation of the subtropical South Pacific derived from hydrographic data. *J. Geophys. Res.*, **103,** 21 443–21 468.

Veronis, G., 1977: Use of tracers in circulation studies. *The Sea*, E. D. Goldberg et al., Eds., Marine Modeling, Vol. 6, Wiley and Sons, 169–188.

Wacogne, S., and R. Pacanowski, 1996: Seasonal heat transport in a primitive equations model of the tropical Indian Ocean. *J. Phys. Oceanogr.*, **26,** 2666–2699.

Walin, G., 1982: On the relation between sea-surface heat flow and thermal circulation in the ocean. *Tellus*, **34,** 187–195.

Webb, D. J., A. C. Coward, B. A. de Cuevas, and C. S. Gwillam, 1997: A multiprocessor ocean general circulation model using message passing. *J. Atmos. Oceanic Technol.,* **14,** 175–183.

——, B. A. de Cuevas, and A. C. Coward, 1998a: The first main run of the OCCAM global ocean model. James Rennell Division Internal Rep. 34, Southampton Oceanography Centre, 50 pp. [Available online at http://www.soc.soton.ac.uk/JRD/OCCAM.]

——, ——, and C. S. Richmond, 1998b: Improved advection schemes for ocean models. *J. Atmos. Oceanic Technol.,* **15,** 1171–1187.

Whitworth, T., B. A. Warren, W. D. Nowlin, S. B. Rutz, R. D. Pillsbury, and M. I. Moore, 1999: On the deep western-boundary current in the Southwest Pacific Basin. *Progress in Oceanography,* Vol. 43, Pergamon, 1–54.

Zalesak, S. T., 1979: Fully multidimensional flux corrected transport algorithms for fluids. *J. Comput. Phys.* **31,** 335–362.